A simple method for analysing the deformation of nanoelectromechanical switches based on carbon nanotubes

Yuantong Gu and Liangchi Zhang*

Mechanical and Mechatronic Engineering,
School of Aerospace,
The University of Sydney,
Sydney, NSW 2006, Australia
Fax: +61-2-9351-7060
E-mail: yuantong.gu@aeromech.usyd.edu.au
E-mail: zhang@aeromech.usyd.edu.au
*Corresponding author

Abstract: This paper developed an effective multiscale method for analysing the deformation of NanoElectroMechanical (NEM) switches based on carbon nanotubes. The switches were simplified to beam systems with loads calculated from three-coupled energy domains: the electrostatic energy domain, the elastostatic energy domain, and the van der Waals energy domain. A meshless formulation was then used to discretise the switches to establish the non-linear system of equations for solution. The pull-in voltage characteristics of the fixed-fixed and cantilever nanoswitches based on the single-walled nanotube and the double-walled nanotube are analysed. A parametric comparison with the results in the literature showed that the method developed in this paper is very effective.

Keywords: nanotechnology; nanotube; NanoElectroMechanical Systems (NEMS); Molecular Dynamics (MD); continuum; meshless method; non-linearity; switch.

Reference to this paper should be made as follows: Gu, Y.T and Zhang, L.C. (2006) 'A simple method for analysing the deformation of nanoelectromechanical switches based on carbon nanotubes', *Int. J. Nanomanufacturing*, Vol. 1, No. 2, pp.210–222.

Biographical notes: Yuantong Gu received his PhD from the National University of Singapore (NUS) in 2003. Currently, he is an Australian Research Council (ARC) Postdoctoral Fellow in the School of Aerospace, Mechanical and Mechatronic Engineering at the University of Sydney. His research interests include nanotechnology, multiscale systems, MicroElectroMechanical Systems (MEMS), NanoElectroMechanical Systems (NEMS), computational mechanics, advanced finite element analysis and modelling, meshfree (meshless) methods, mechanical and ship engineering, high performance computing techniques and dynamic and static analyses of structures.

Liangchi Zhang is a Professor at the University of Sydney, Australia. He received a BSc, an ME and a PhD in Solid Mechanics in China, in 1982, 1985 and 1988, respectively. He then worked as a Postdoctoral Research Assistant (1989–1991) at the University of Cambridge, UK, on contact mechanics, and an STA Fellow (1991–1992) at MEL Japan on grinding.

He joined the University of Sydney in July 1992 and has been working in the areas of nanomechanics and nanomaterials, tribology, solid mechanics and machining. He was awarded Doctor of Engineering by the University of Sydney in 2005. His research activities can be found at http://nt-542.aeromech.usyd.edu.au/.

1 Introduction

Manufacturing has always been a major wealth-creating sector in developed economies and will be the cornerstone of long-term economic growth in the world. The design and manufacturing of MicroElectroMechanical Systems (MEMS) have become very important (Bhushan, 2005) because of the accelerating role of MEMS in automotive systems (transducers and accelerometers), avionics and aerospace (microscale actuators and sensors), manufacturing and fabrication (micro smart robots), medicine and bioengineering (DNA and genetic code analysis and synthesis, drug delivery, diagnostics and imaging), and so on. The increasing interest in nanotechnology has also influenced the development of MEMS. A new class of MEMS devices being developed at the nanoscale is called NanoElectroMechanical Systems (NEMS). The NEMS device is about a thousand times smaller than MEMS, and has a promising potential in practical applications in, for example, random access memories (Rueckes et al., 2000), nanotweesers for miniaturised robots (Kim and Lieber, 1999), and nanoswitches (Baughman et al., 1999), where carbon nanotubes are often used because of their excellent electronic, chemical and mechanical properties (Mylvaganam and Zhang, 2004a,b). In these NEMS, the carbon nanotube-based switch is a very important group of NanoElectroMechanical (NEM) devices due to its wide practical applications.

Due to their smaller dimensional scale, experiments on nanoswitches are costly. Numerical simulations have therefore become an important tool for their analysis and design. A common and powerful approach related to nanoscale simulation is the Molecular Dynamics (MD) (Dequesnes et al., 2004; Rapaport, 1995), which can be used to simulate the static and dynamic behaviour of nanoswitches. However, MD simulations require the computation of many atoms in the system, making it unrealistic for studying large and complex systems. To overcome this difficulty, an effective alterative approach should be developed.

In recent years, a group of advanced numerical techniques, the meshless methods (Gu, 2005; Liu, 2002; Liu and Gu, 2005), have been developed and achieved remarkable progress for the continuum analysis. The meshless methods using various weak-forms of the Ordinary Differential Equations (ODEs) or the Partial Differential Equations (PDEs) of the problems, for example, the Element-Free Galerkin (EFG) method (Belytschko et al., 1994), the Meshless Local Petrov-Galerkin (MLPG) method (Atluri and Zhu, 1998), and the Local Radial Point Interpolation Method (LRPIM) (Gu and Liu, 2001; Liu and Gu, 2001), have shown many distinguished advantages in the applications for engineering and sciences. These advantages include no mesh generation, high accuracy, easy for adaptive analysis and so on. Especially, the meshless methods perform better in solving some non-linear, large deformation, and multiple domains coupled problems, which are usually difficult to be solved using the traditional numerical methods, for example, the Finite Element Method (FEM).

This paper will develop a new method for characterising the deformation of two typical NEM switches, as shown in Figures 1 and 2, whose key components are a Single-Walled carbon NanoTube (SWNT) or a Double-Walled carbon NanoTube (DWNT) and a fixed ground plane. When a potential difference is created between the nanotube and the ground plane, electrostatic charges, which will lead to electrostatic force, are introduced. Meanwhile, elastostatic and van der Waals forces coexist. Under an applied voltage, an equilibrium position of the tube is defined by the balance of the elastostatic, electrostatic and the van der Waals forces. To simulate these NEM switches, a parameterised continuum model will be used, in which the Young's modulus and moment of inertia of the SWNT will be obtained by the analytical method based on the values obtained by Vodenitcharova and Zhang (2003), and the product of Young's modulus and moment of inertia of the DWNT will be determined by MD simulation with a linear deflection approximation. The switch will be simplified to a beam system, and the loading be calculated from three coupled energy domains: the electrostatic energy domain, the elastostatic energy domain, and the van der Waals energy domain. A meshless formulation (Gu and Liu, 2001; Liu and Gu, 2005) will then be developed to discretise the domain of the switch to establish the non-linear equations for deformation analysis. The pull-in voltage characteristics of fixed-fixed and cantilever nanoswitches based on the SWNT and the DWNT are analysed.

Figure 1 A fixed-fixed NEM based switch (a) voltage $V = 0$ and (b) voltage $V > 0$

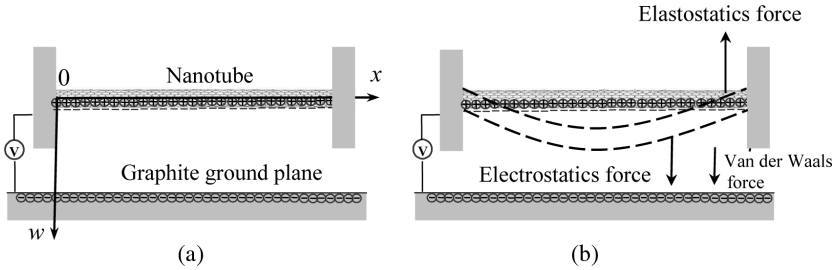

Figure 2 A cantilever NEM based switch (a) voltage $V = 0$ and (b) voltage $V > 0$

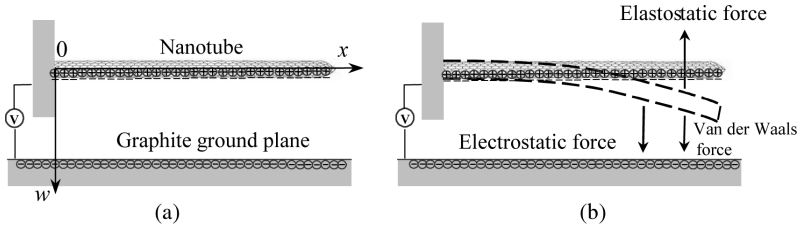

2 Modelling

2.1 The elastostatic domain

When the deflection of the nanotube is small and its cross-section shape change during bending is negligible, the nanotube in the switch can be simplified to a beam structure. According to the continuum theory, the governing equation for the beam can be written as (Zienkiewicz and Taylor, 2000)

$$EI\frac{d^4w}{dx^4} = f \tag{1}$$

where w is the deflection of the nanotube, E is its Young's modulus, I is its moment of inertia, and f is the force per unit length on the tube.

For a tube shown in Figures 1 and 2, there are four boundary conditions, two at each end. The boundary conditions are given at the global boundary, Γ, as

$$w(0) = 0,\ \theta(0) = 0,\ w(l) = 0,\ \theta(l) = 0, \text{ for a fixed-fixed tube} \tag{2}$$

$$w(0) = 0,\ \theta(0) = 0,\ M(l) = 0,\ Q(l) = 0, \text{ for a cantilever tube} \tag{3}$$

where θ, M and Q denote the deflection slope, the bending moment and the shear force, respectively, and l is the length of the tube.

2.2 The electrostatic force

The electrostatic force can be computed by using a standard capacitance model (Jackson, 1998), in which the nanotube is considered as a perfect cylindrical conductor. This implies that the potential is constant along the length of the tube. The capacitance per unit length for the cylindrical beam over a conductive ground plane is given by Jackson (1998) and Dequesnes et al. (2004)

$$C(r) = \frac{2\pi\varepsilon_0}{\log\left[1 + g/r_1 + \sqrt{(g/r_1 + 1)^2 - 1}\right]} \tag{4}$$

where ε_0 is the permittivity at vacuum, g is the gap between the nanotube and ground plane, and r_1 is the radius of the conductor (i.e. the exterior radius of the tube). These parameters are more clearly defined in Figures 3 and 4.

Figure 3 A SWNT over a graphite ground plane

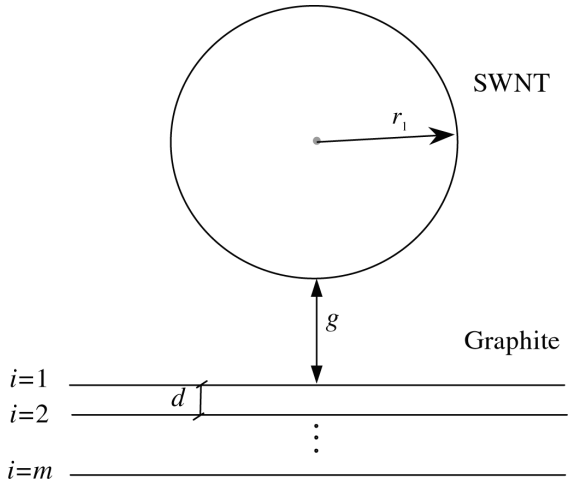

Figure 4 A DWNT over a graphite ground plane

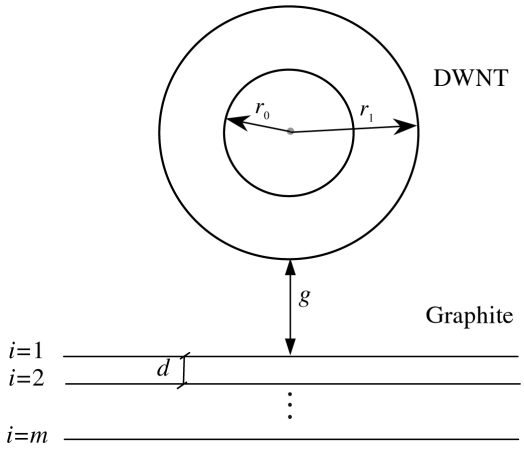

The electrostatic energy per unit length is given by

$$\Phi_{\text{elec}} = \frac{1}{2}C(r)V^2 \tag{5}$$

where V is the voltage applied. Therefore, the electrostatic force per unit length can be written as

$$\begin{aligned} f_1 &= \frac{d\Phi_{\text{elec}}}{dr} \\ &= -\pi\varepsilon_0 V^2 \left\{ r_1 \left[\frac{g\left(g+2r_1\right)}{r_1^2} \right]^{1/2} \log^2 \left\{ 1 + \frac{g}{r_1} + \left[\frac{g\left(g+2r_1\right)}{r_1^2} \right]^{1/2} \right\} \right\}^{-1} \end{aligned} \tag{6}$$

2.3 The van der Waals interaction

The van der Waals force can be computed through the van der Waals energy, which describes the interaction of nanotube with ground plane, using an atomistic potential. The following Lennard-Jones (L-J) potential is used in this paper (Rapaport, 1995)

$$\Phi\left(\mathbf{r}_{ij}\right) = 4\varepsilon\left[\left(\frac{\sigma}{\mathbf{r}_{ij}}\right)^{12} - \left(\frac{\sigma}{\mathbf{r}_{ij}}\right)^{6}\right] = \frac{4\varepsilon\sigma^{12}}{\mathbf{r}_{ij}^{12}} - \frac{4\varepsilon\sigma^{6}}{\mathbf{r}_{ij}^{6}} = \frac{C_{12}}{\mathbf{r}_{ij}^{12}} - \frac{C_6}{\mathbf{r}_{ij}^{6}} \tag{7}$$

where C_{12} and C_6 are constants characterising the interactions between two atoms. In the L-J potential, there are attractive and repulsive parts. The repulsive part decays very fast and plays an important role only when the nanotube is to contact with the ground. Since the major aim of this paper is to calculate the pull-in voltages, which leads to a deflection before contacting, it is reasonable to only consider the attractive part in the calculation of the van der Waals energy W using a pair-wise summation over all the atoms. As shown in Figure 3, when a SWNT interacts with m layers of grapheme in the substrate, and if the interlayer distance of the grapheme is d, the van der Waals force of the SWNT can be written as (Dequesnes et al., 2003)

$$f_2 = -\sum_{i=1}^{m} \frac{\left[C_6\sigma_0^2\pi^2 r_1\sqrt{g_i\left(g_i+2r_1\right)}\right]\left(8g_i^4+32g_i^3r_1+72g_i^2r_1^2+80g_ir_1^3+35r_1^4\right)}{2g_i^5\left(g_i+2r_1\right)^5} \tag{8}$$

where σ_0 is the graphite surface density, $g_i = g + d \times (i-1)$, and r_1 is the radium of the SWNT.

Similarly, as shown in Figure 4, when a DWNT interacts with m layers of grapheme in the substrate, and if the interlayer distance of the grapheme is d, the van der Waals force of the DWNT can be written as (Dequesnes et al., 2003)

$$\begin{aligned} f_2 = -\sum_{i=1}^{m}\Bigg\{ & \frac{\left[C_6\sigma_0^2\pi^2 r_1\sqrt{g_i\left(g_i+2r_1\right)}\right]\left(8g_i^4+32g_i^3r_1+72g_i^2r_1^2+80g_ir_1^3+35r_1^4\right)}{2g_i^5\left(g_i+2r_1\right)^5} \\ & + \frac{\left[C_6\sigma_0^2\pi^2 r_0\sqrt{g_i\left(g_i+2r_0\right)}\right]\left(8g_i^4+32g_i^3r_0+72g_i^2r_0^2+80g_ir_0^3+35r_0^4\right)}{2g_i^5\left(g_i+2r_0\right)^5}\Bigg\} \end{aligned} \tag{9}$$

where r_0 and r_1 are the radii of the inner and outer nanotubes of the DWNT.

The total force in Equation (1), f, is therefore

$$f = f_1 + f_2 \tag{10}$$

3 Young's modulus and moment of inertia

To use the continuum model, Young's modulus, E, and moment of inertia, I, of the nanotube must be determined. There have been some confusions in determining the Young's modulus (Wong et al., 1997) of a nanotube due to the dilemma of the effective thickness, h. For example, some studies assumed that a nanotube was a solid cylinder. Others considered that h was equal to the interplanar spacing of graphite layer, that is, h_g = 3.4 Å. Therefore, the equivalent Young's modulus calculated based on these h values varies. Vodenitcharova and Zhang (2003) clarified the dilemma and formulated the effective thickness. They pointed out that the equivalent thickness of a SWNT is 0.617 Å, which is 43.8% of the theoretical diameter of a carbon atom, and its Young's modulus is 4.88 TPa.

3.1 SWNT

The values of E and h obtained by Vodenitcharova and Zhang (2003) was used for the SWNT in this paper, that is, Young's modulus E = 4.88 TPa. The moment of inertia, I, can be obtained based on the equivalent thickness h

$$I = \frac{\pi}{4}\left[\left(R+\frac{h}{2}\right)^4 - \left(R-\frac{h}{2}\right)^4\right] \tag{11}$$

where h = 0.617 Å is the equivalent thickness (Vodenitcharova and Zhang, 2003) and R is the radius of the tube's mid-surface, that is, the one through the centre of the carbon atoms.

3.2 DWNT

There is not a rational value of wall-thickness for a DWNT that can be used to determine its E and I. Since this study considers only the linear elasticity of the DWNT with small deflection, its E and I are therefore constants. Hence, the linear deflection approximation, in which the peak deflection of the tube is considered as a linear function of the applied load, can be used to get the product of E and I. The peak deflections for different loadings are first obtained by the MD simulation, and then using the classic beam theory to calculate EI. That is, for a cantilever or fixed-fixed tube, if the peak deflection is w_{d} (obtained by MD simulation (Dequesnes et al., 2003; Mylvaganam and Zhang, 2004c) when the force is f, we can simply obtain EI as

$$EI = \frac{l^4 f}{8 w_d}, \quad \text{for a cantilever tube} \tag{12}$$

$$EI = \frac{l^4 f}{384 w_d}, \quad \text{for a fixed-fixed tube} \tag{13}$$

where l is the length of the tube. To ensure the accuracy, various loading conditions can be used to get several values of EI, and the average of these values EI can be taken as the equivalent EI.

4 Local meshless formulation

A local weak form of the differential Equation (1), over a local domain Ω_q bounded by Γ_q, can be obtained using the local weighted residual method (Gu and Liu, 2001; Liu and Gu, 2005)

$$\int_{\Omega_q} \hat{w}\left(EIw'''' - f\right)\mathrm{d}x = 0 \tag{14}$$

where $\hat{w}$ is the weight function. The first term on the left hand side of Equation (14) can be integrated by parts to become

$$\int_{\Omega_q} \left(EI\hat{w}''w'' - \hat{w}f\right)\mathrm{d}x - \left[\bar{n}EI\hat{w}'w''\right]_{\Gamma_q} + \left[\bar{n}EI\hat{w}w'''\right]_{\Gamma_q} = 0 \tag{15}$$

where $\bar{n}$ is the unit outward normal to domain Ω_q.

An arbitrary shape quadrature domain can be used, such as a linear support domain for one-dimensional problems. It can be found that the boundary Γ_q for the support domain usually comprises five parts: the internal boundary Γ_{qi}, the boundaries Γ_{qw}, $\Gamma_{q\theta}$, Γ_{qM}, and Γ_{qQ}, over which the essential boundary conditions w, θ and natural boundary conditions M, Q are specified. The boundaries Γ_{qw} with Γ_{qQ} and $\Gamma_{q\theta}$ with Γ_{qM} are mutually disjoint. Imposing the natural (force) boundary condition given in Equations (2) and (3), we obtain:

$$\begin{aligned}\int_{\Omega_q} \left(EI\hat{w}''w'' - \hat{w}f\right)\mathrm{d}x - \left[\bar{n}\bar{M}\hat{w}'\right]_{\Gamma_{qM}} - \left[\bar{n}\bar{Q}\hat{w}\right]_{\Gamma_{qQ}} - \left[\bar{n}EI\hat{w}'w''\right]_{\Gamma_{q\theta}} \\ + \left[\bar{n}\hat{w}EIw'''\right]_{\Gamma_{qw}} - \left[\bar{n}\hat{w}'EIw''\right]_{\Gamma_{qi}} + \left[\bar{n}\hat{w}EIw'''\right]_{\Gamma_{qi}} = 0\end{aligned} \tag{16}$$

If the value and the derivatives of the weight function $\hat{w}$ are taken to be zero at Γ_{qi}, the last two terms in Equation (16) vanish.

Gauss quadrature is needed to evaluate the integrations in Equation (16). As shown in Figure 5, for a field node x_I, a local quadrature cell Ω_q is needed for the Gauss quadrature; for each Gauss quadrature point x_Q, the meshless shape functions are constructed to obtain the integrand. Therefore, for a field node x_I, there exists three local domains:

- the local quadrature domain Ω_q (size r_q)
- the local weight (test) function domain Ω_w where $\hat{w}_i \neq 0$ (size r_w) and
- the local support domain Ω_s for x_Q (size r_s).

Figure 5 The weight domain Ω_v and quadrature domain Ω_q for node *I*; support domain Ω_s for Gauss integration point x_Q

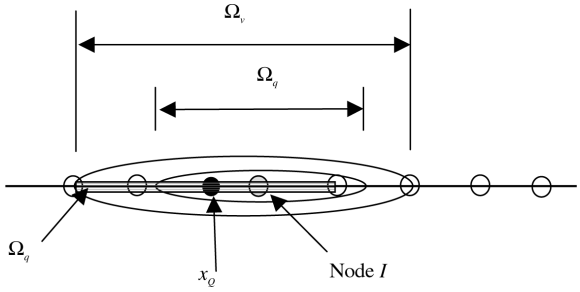

These three local domains are arbitrary as long as the condition $r_q \leq r_w$ is satisfied. It has been noted that when an appropriate weight function is used, the local weak form, Equation (16), can be simplified because the terms along the internal boundary vanish. Hence, for simplicity, we can use $r_q = r_w$.

The problem domain Ω is represented by properly scattered field nodes, and the Hermite point interpolation (Liu and Gu, 2005) is used to approximate the value of a point x

$$w(x) = \mathbf{\Phi}_w^{\mathrm{T}}(x)\mathbf{w} + \mathbf{\Phi}_\theta^{\mathrm{T}}(x)\boldsymbol{\theta} \tag{17}$$

where $\mathbf{w}$ and $\boldsymbol{\theta}$ denote the nodal deflections and slopes, respectively, and $\mathbf{\Phi}_w(x)$ and $\mathbf{\Phi}_\theta(x)$ are shape functions for deflection and slope, respectively.

As this local meshless method is regarded as a weighted residual method, the weight function plays an important role in the performance of the method. It can be found that a weight function with the local property will yield better results, such as the quartic spline function. Following the idea of the Galerkin FEM, the weight function $\hat{w}$ can be taken as

$$\hat{w}\left(x_Q\right) = \boldsymbol{\psi}_w^{\mathrm{T}}(x)\boldsymbol{\alpha} + \boldsymbol{\psi}_\theta^{\mathrm{T}}(x)\boldsymbol{\beta} \tag{18}$$

where $\boldsymbol{\alpha}$ and $\boldsymbol{\beta}$ denote the fictitious nodal coefficients, $\mathbf{\Psi}_w$ and $\mathbf{\Psi}_\theta$ are constructed using meshless shape functions. It should be noted that the support domain used to construct $\mathbf{\Psi}_w$ and $\mathbf{\Psi}_\theta$ can be independent of the support domain used to construct $\mathbf{\Phi}_w$ and $\mathbf{\Phi}_\theta$.

Substituting Equations (17) and (18) into the local weak form Equation (16) for all nodes leads to the following discrete equations

$$\mathbf{K}\mathbf{w}^e = \mathbf{f} \tag{19}$$

It can be found from Equations (6), (8) and (9) that f is non-linear, because it is the function of the deflection. The non-linear force f leads to the non-linearity of Equation (19), and thus an iteration technique, the Newton-Raphson method in the present case, is required for its solution. The simple iteration criteria is defined as

$$\sqrt{\frac{\sum_{j=1}^{n}\left(w_j^{i+1}-w_j^{i}\right)^2}{\sum_{j=1}^{n}\left(w_j^{i+1}\right)^2}} \le e \tag{20}$$

where n is the number of nodes used, w_j^i and w_j^{i+1} are the deflections of the ith and the (i+1)th iteration steps, respectively, and e is a specified accuracy tolerance.

5 Results and discussions

5.1 A cantilever DWNT-based switch

A cantilever switch is considered to consist of a DWNT of 50 nm in length, with $r_1 = 1$ nm, and $r_0 = 0.665$ nm. The initial gap between the DWNT and the ground plane is 4 nm. There are 30 sheets of grapheme for the ground plane, and the inter-layer distance of graphite, d, is 0.335 nm. The equivalent product of EI is $7.58 \times 10^{-25}\text{m}^2\text{N}$ and $\varepsilon_0 = 8.854 \times 10^{-12}\text{C}^2\text{N/m}^2$ (Jackson, 1998).

To analyse this switch by the above meshless formulation, 41 regularly distributed field nodes are used. It can be found that with the increase of the applied voltage, the deflection of the DWNT increases, and the gap between the tube and the ground plane decreases. When the voltage increases to a certain value, the tube becomes unstable suddenly and the free end of the tube will touch the bottom plane. This process is defined as the pull-in behaviour (Wang et al., 2004) and the corresponding voltage value is called the quasi-static critical pull-in voltage, at which the deflection of the tube tip equals the initial gap. In the practical applications of NEM switches, the critical pull-in voltage is one of the most important parameters.

Figure 6 demonstrates the result of the deflection of this DWNT tube tip under different voltages. It can be seen that the critical pull-in voltage is 0.474 volt. Compared with the same value, 0.5 volt, obtained by an analytical method (Dequesnes et al., 2003; Osterberg, 1995), the presented method gives a very good result. It should be mentioned here that the above model is only valid when the tube deflection is small. However, it can be seen from Figure 6 that the model is accurate up to the critical pull-in voltage. The sharp increase of the tube deflection beyond the critical pull-in voltage, as shown in Figure 6, is caused by the sharp increase of the forces, as demonstrated in Figure 7. Because of the decrease of the gap between the DWNT and the ground plane, both the electrostatic and van der Waals forces increase significantly, which pull the tube down suddenly. To simulate the deflection process after the critical pull-in voltage, a geometrically non-linear model must be developed.

Figure 6 The gap under different voltages for the cantilever DWNT based switch

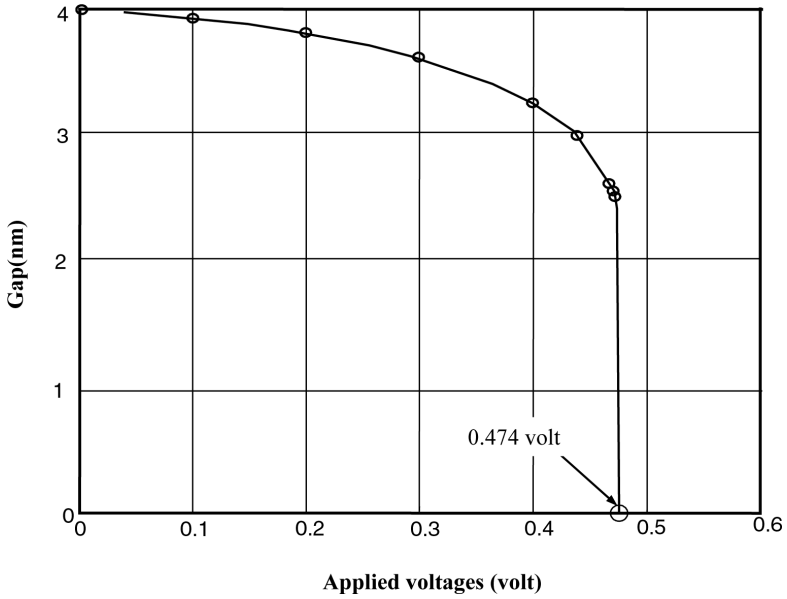

Figure 7 Forces versus gaps for the cantilever DWNT based switch

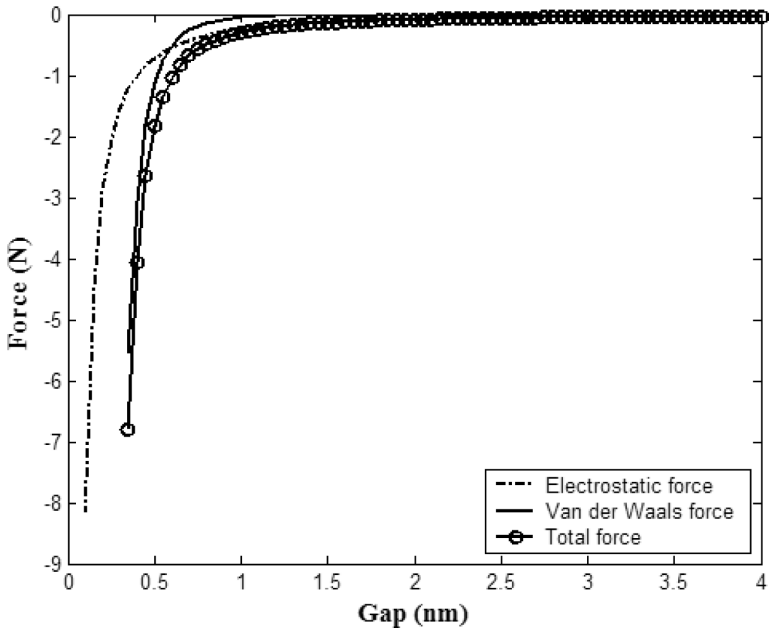

Figure 8 demonstrates the relationship between the critical pull-in voltage and the initial gap for this switch. It clearly shows that the critical pull-in voltage increases with the increase of the initial gap. When the initial gap is larger than 6 nm, the slope for the curve changes very slowly, because with a large gap the effect of the van der Waals

force is negligible. When the gap is very small, on the other hand, the van der Waals force will play a key role. At a critical gap value ($g \approx 3.5$ nm in the present case), pull-in will occur even without an external voltage.

Figure 8 Pull-in voltages versus gaps for the cantilever DWNT based switch

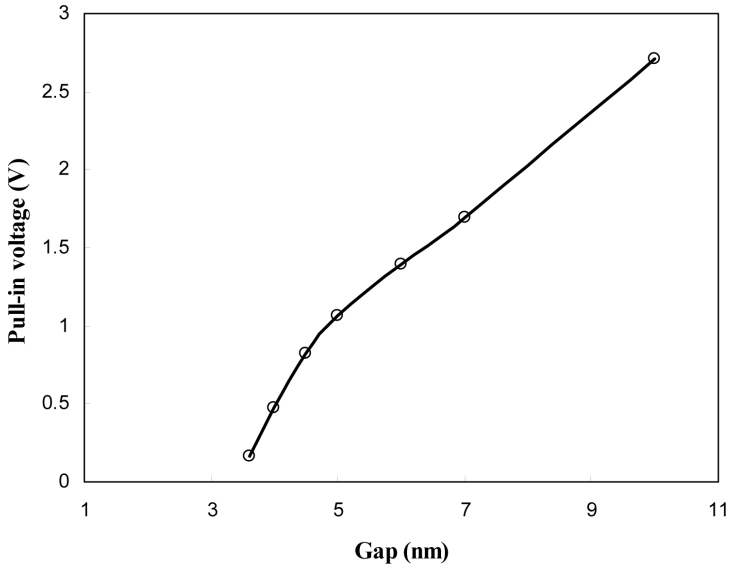

A fixed-fixed switch based on the same DWNT is also simulated. All computational parameters are the same as those listed above. The critical pull-in voltage obtained now becomes 6.15 V, which is much higher than that of the cantilever switch. This is understandable because the fixed-fixed boundary conditions make the tube much stiffer.

5.2 A fixed-fixed SWNT-based switch

A fixed-fixed SWNT-based switch is also considered to consist of a SWNT of 20.7 nm in length, with $r_1 = 0.665$ nm. The initial gap between the DWNT and the ground plane is 2 nm. There are 40 sheets of grapheme for the ground plane, and the inter-layer distance of graphite, d, is 0.335 nm. The permittivity of vacuum equivalent ε_0 is $8.854 \times 10^{-12}\text{C}^2\text{N/m}^2$. Using Equation (11) and the value $E = 4.88$ TPa with effective thickness $h = 0.617$ Å (Vodenitcharova and Zhang, 2003), we get $EI = 2.5 \times 10^{-25}\text{m}^2\text{N}$, which is very close to the result $2.3 \times 10^{-25}\text{m}^2\text{N}$ (Dequesnes et al., 2004) obtained by MD.

To analyse this switch by the above meshless formulation, 21 regularly distributed field nodes are used. With the increase of the applied voltage, the deflection of the SWNT increases, and the gap between the tube and the ground plane decreases. When the voltage increases to a certain value, the tube also becomes unstable suddenly, which is similar to the switch in the first example, and the middle of the tube will touch the bottom plane. The corresponding quasi-static critical pull-in voltage can be obtained from Figure 9, which demonstrates the result of the deflection of the tube tip under different voltages. For this switch, it can be found that the critical pull-in voltage is 9.07 vol.

Figure 9 The gap under different voltages for the fixed-fixed SWNT based switch

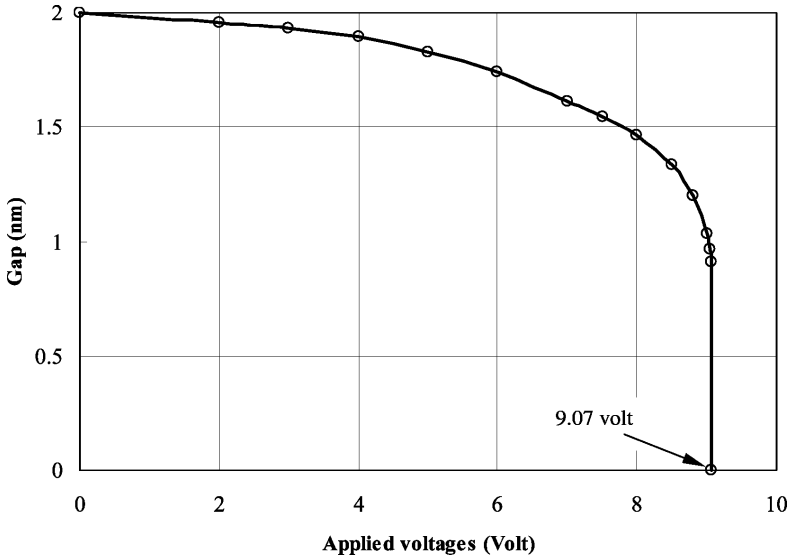

6 Conclusion

This paper has analysed the deformation of some NEM switches using the meshless technique based on a parameterised continuum model. The pull-in voltage characteristics of fixed-fixed and cantilever nanoswitches based on the single-walled nanotube and the double-walled nanotube are studied. From studies of this paper, the following conclusions can be drawn:

1 The proposed technique is very simple and effective to give satisfactory results for NEM switches.

2 The coupling of elastostatic and van der Waals forces is important when the gap between the tube and the ground is not too small but not too big.

3 The presented model is only valid when the tube deflection is small and it is usually accurate up to the critical pull-in voltage. However, to analyse the deflection process after the critical pull-in voltage, a geometrically non-linear model must be developed.

Acknowledgement

This work was supported by an Australian Research Council (ARC) Discovery Grant.

References

Atluri, S.N. and Zhu, T. (1998) 'A new meshless local petrov-galerkin (MLPG) approach in computational mechanics', *Computational Mechanics*, Vol. 22, pp.117–127.

Baughman, R.H., et al. (1999) 'Carbon nanotube actuators', *Science*, Vol. 284, pp.1340–1344.

Belytschko, T., Lu, Y.Y. and Gu, L. (1994) 'Element-free galerkin methods', *International Journal for Numerical Methods in Engineering*, Vol. 37, pp.229–256.

Bhushan, B. (2005) *Nanotribology and Nanomechanics*, Berlin: Springer.

Dequesnes, M., Rotkin, S.V. and Aluru, N.R. (2003) 'Calculation of pull-in voltages for carbon-nanotube-based nanoelectromechanical switches', *Nanotechnology*, Vol. 13, pp.120–131.

Dequesnes, M., Tang, Z. and Aluru, N.R. (2004) 'Static and dynamic analysis of carbon nanotube-based switches', *Journal of Engineering Materials and Technology*, Vol. 126, pp.230–237.

Gu Y.T. (2005) 'Meshfree methods and their comparisons', *International Journal of Computational Methods (IJCM)*, in Y.T. Gu and W. Kanok-Nukulchai (Eds). Vol. 2, No. 4, pp.477–515.

Gu, Y.T. and Liu, G.R. (2005) 'A local point interpolation method for static and dynamic analysis of thin beams', *Computer Method in Applied Mechanics Engineering*, Vol. 190, pp.5515–5528.

Jackson, J.D. (1998) *Classical Electrodynamics*, 3rd edition, NewYork: Wiley.

Kim, P. and Lieber, C.M. (1999) 'Nanotube nanotweezers', *Science*, Vol. 286, pp.2148–2150.

Liu, G.R. (2002) *Mesh Free Methods: Moving Beyond the Finite Element Method*, USA: CRC press.

Liu, G.R. and Gu, Y.T. (2001) 'A local radial point interpolation method (LR-PIM) for free vibration analyses of 2-D solids', *Journal of Sound and Vibration*, Vol. 246, No. 1, pp.29–46.

Liu, G.R. and Gu, Y.T. (2005) *An Introduction to Meshfree Methods and Their Programming*, Berlin: Springer.

Mylvaganam, K. and Zhang, L.C. (2004a) 'Chemical bonding in polyethylene-nanotube composites: a quantum mechanics prediction', *Journal of Physical Chemistry B*, Vol. 108, pp.5217–5220.

Mylvaganam, K. and Zhang, L.C. (2004b) 'Nanotube functionalization and polymer grafting: an ab initio study', *Journal of Physical Chemistry B*, Vol. 108, pp.15009–15012.

Mylvaganam, K. and Zhang, L.C. (2004c) 'Important issues in a molecular dynamics simulation for characterizing the mechanical properties of carbon nanotubes', *Carbon*, Vol. 42, pp.2025–2032.

Osterberg, P.M. (1995) 'Electrostatically actuated micromechanical test structures for material property measurement', PhD Dissertation, Cambridge, MA: MIT.

Rapaport, D.C. (1995) *The Art of Molecular Dynamics Simulation*, Cambridge University Press.

Rueckes, T., et al. (2000) 'Carbon nanotube-based nonvolatile random access memory for molecular computing', *Science*, Vol. 289, pp.94–97.

Vodenitcharova, T. and Zhang, L.C. (2003) 'Effective wall thickness of a single-walled carbon nanotube', *Physcial Review B*, Vol. 68, pp.165–401.

Wang, Q.X., et al. (2004) 'Analysis of microelectromechanical systems (MEMS) by meshless Local Kriging (LoKriging) method', *Journal of the Chinese Institute of Engineers*, Vol. 27, pp.573–583.

Wong, E.W., Sheehan, P.E. and Lieber, C.M.V. (1997) 'Nanobeam mechanics: elasticity, strength, and toughness of nanorods and nanotubes', *Science*, Vol. 277, pp.1971–1975.

Zienkiewicz, O.C. and Taylor, R.L. (2000) *The Finite Element Method*, 5th edition, Oxford: Butterworth Heinemann.